The Journal of Veterinary Medical Science

NOTE

Surgery

Cortical laminar necrosis detected by diffusion-weighted imaging in a dog suspected of having hypoglycemic encephalopathy

Ai HORI[1)], Kenjirou MIYOSHI[1)], Wakako SEO[1)], Ako KAKUTA[1)], Kiwamu HANAZONO[1)] and Tetsuya NAKADE[1)]*

[1)]Department of Small Animal Clinical Sciences, School of Veterinary Medicine, Rakuno Gakuen University, 582-1 Bunkyoudai-Midorimachi, Ebetsu, Hokkaido 069-8501, Japan

J. Vet. Med. Sci.
82(12): 1763–1768, 2020
doi: 10.1292/jvms.20-0134

Received: 11 March 2020
Accepted: 15 October 2020
Advanced Epub:
2 November 2020

ABSTRACT. We describe a 5-year-old castrated male dog suspected hypoglycemic encephalopathy that was evaluated by using diffusion-weighted imaging (DWI). The dog experienced hypoglycemia after prolonged generalized and continued partial seizures. In the acute phase, DWI showed hyperintensity in the left temporal lobe. After about a month, DWI maintained hyperintensity, and left middle cerebral artery dilation was noted on magnetic resonance angiography (MRA). In the chronic phase, the left temporal lobe lesion was replaced by cerebrospinal fluid. In humans, it was reported that cortical laminar necrosis (CLN) with hypoglycemic encephalopathy presents hyperintensity in the cerebral cortex on DWI and increased vascularity of the middle cerebral artery branches on MRA. In conclusion, DWI has detected CLN in a dog suspected hypoglycemic encephalopathy.

KEY WORDS: diffusion-weighted imaging, hypoglycemic encephalopathy, magnetic resonance imaging

Cortical laminar necrosis (CLN) is observed as necrosis in the cerebrocortical gray matter and occurs due to numerous encephalopathy etiologies [2, 3, 11, 12, 14–16, 18–20], including ischemic stroke, generalized seizures, hypoglycemia, and hypoxia [2, 3, 14, 18, 20]. CLN is supported when magnetic resonance imaging (MRI) findings indicate diffuse cortical injury [2, 11, 12, 14–16, 19–20]. In humans, some reports recommend that additional scans, such as diffusion-weighted imaging (DWI), are helpful to diagnose the acute encephalopathy cause [1, 4, 9, 10, 12, 13, 16]. DWI shows a typical high signal intensity at the early stages of CLN, and is more sensitive than T2-weighted imaging (WI) or fluid attenuated inversion recovery (FLAIR) [9, 10, 12, 13]. As in humans, there are reports on the use of MRI in patients with CLN [2, 3, 14, 15, 18, 20]. In a dog with CLN after general anesthesia, the cerebral cortex was observed as linear hyperintensity on T1WI, and T1WI with heterogeneous contrast enhancement [2]. In the report, the lesion, suspected to have arisen from a hypoxic event, was detected as increased signal intensity on DWI that was performed during the late subacute phase [2]. Although there are reports on detecting CLN by MRI, there are few reports on clinical CLN cases detected by DWI during the acute phase. Herein, we report a case of a dog with hypoglycemia-associated CLN after status epilepticus, and describe the MRI findings over 4 months.

We report a case of a mixed breed, 5-year-old, castrated male dog, weighing 2.5 kg. The dog had experienced over ten episodes of generalized and cluster epileptic seizures during a 2-hr period. While at a nighttime emergency animal hospital, it received intravenously (IV) 0.5 mg/kg diazepam (Horizon Injection 10 mg®, Maruishi Pharmaceutical, Osaka, Japan) and 30 mg/kg levetiracetam (LEV) (E Keppra for IV infusion 500 mg®, UCB Japan, Tokyo, Japan), subcutaneously 1.0 mg/kg prednisolone (Predonizoron Injection KS®, Kyoritsu Seiyaku, Osaka, Japan), and continuous-rate infusion (CRI) of 1.0 g/kg mannitol (Mannitol injection YD®, Yokushindou Co., Ltd., Toyama, Japan) for 30 min. Blood tests indicated metabolic acidosis and dehydration: pH, 7.24; partial pressure of CO_2 (pCO_2), 40 mmHg; HCO_3^- concentration, 17.1 mmol/l; base excess [BE], −10.3 mmol/l, packed cell volume (PCV); 61.2%. The venous blood gas analysis was performed without correction for temperature (37.0°C). There was no hypoglycemia (Glucose [Glu]: 196 mg/100 ml). Although generalized seizures were absent, partial seizures were observed. Following a loss of consciousness and stiffening of the extremities, the left side of the face exhibited involuntary twitching.

On the second day after onset, the dog was referred to the Animal Medical Center at Rakuno Gakuen University. There was no other medical history. The dog was stuporous, and partial status epilepticus continued for about 31 hr. Neurological examination

*Correspondence to: Nakade, T.: tnakade@rakuno.ac.jp

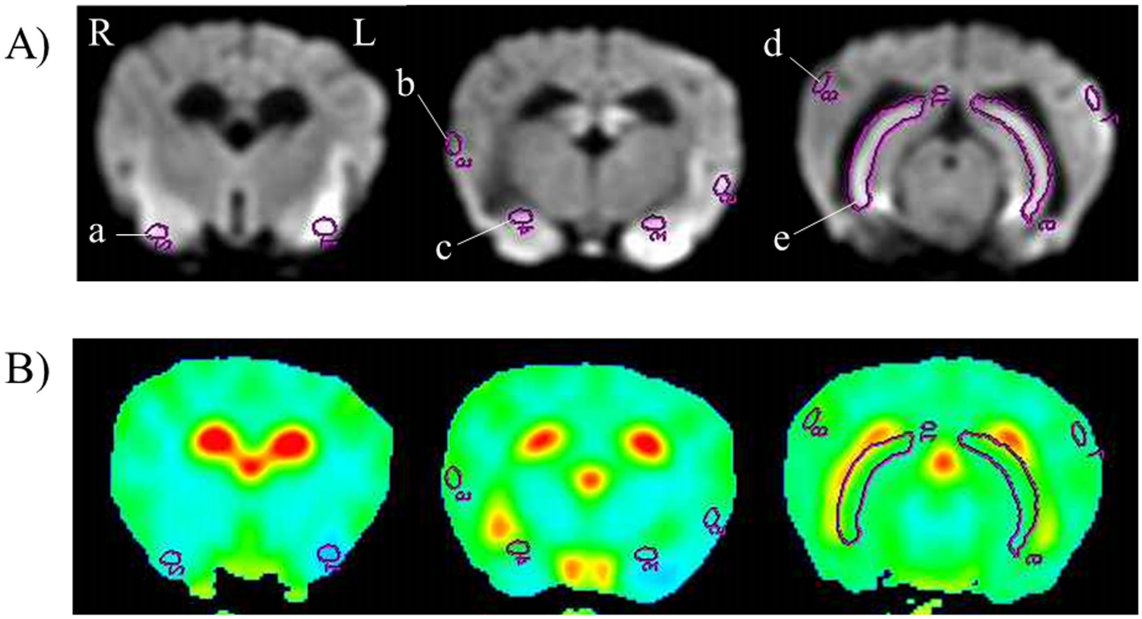

Fig. 1. The region of interest (ROI) locations for the apparent diffusion coefficient (ADC) values. A) These images were DWI. The ROI was set on the piriform lobe (a), gyrus sylvius (b), amygdala (c), gyrus ectosylvius medialis (d), and hippocampus (e). DWI, diffusion-weighted imaging; L, left side; R, right side. B) These images were ADC maps. The ADC values were observed by these images.

showed decreased response to palpebral, corneal, and pupillary light reflexes; sensation; and menace. Anisocoria was observed. On physical examination, hyperthermia (39.7°C) and tachycardia (heart rate: 215 beats/min) were noted. Blood pressure could not be measured because it was too low. Venous blood gas analysis indicated metabolic acidemia: pH, 6.99; pCO_2, 71 mmHg; HCO_3^-, 16.3 mmol/l; and BE, −16.1 mmol/l. Complete blood count and biochemical analysis suggested dehydration, myopathy, hypoglycemia, and acute renal failure: white blood cell count, 26,600/µl; PCV, 69.6%; tissue plasminogen, 8.8 g/100 ml; aspartate aminotransferase (AST), 254 IU/l; alkaline phosphatase (ALP), 2,084 IU/l; blood urea nitrogen, 70.8 mg/100 ml; creatinine, 4.69 mg/100 ml; creatinine kinase (CK), 2,648 IU/l; Glu, 33 mg/100 ml; phosphoric acid, 20.1 mg/100 ml; Na, 161 mmol/l; K, 6.4 mmol/l; and C-reactive protein (CRP), 20.3 mg/100 ml. The dog was cooled; 50% glucose (1 ml/kg), diluted in saline, was injected IV twice, and fluid (isotonic saline solution with 2.5% glucose) was administered IV as a 10-ml/kg bolus and then as CRI at 10–15 ml/kg/hr. Additionally, 20 ml of 0.3 mol/l tris (hydroxymethyl) aminomethane was administered over 2 hr.

Because of the dog's severe condition, 1.5-Tesla MRI was performed without general anesthesia, using a 4-channel surface coil (SIGNA Creator®, 4-channel Flexible Small coil®, GE Medical Systems, Milwaukee, TN, USA). T2-weighted first spin-echo sequence (repetition time [TR], 3,300–4,000 msec; echo time [TE], 105–107 msec; slice thickness, 3.0–4.0 mm), FLAIR (TR, 6800 msec; TE, 94–105 msec), and pre- and post- contrast enhanced T1WI (TR, 360–420 msec; TE, 11–12 msec) images were acquired. Gadobutrol 0.01 mmol/l (Gadovist®, Bayer Yakunin, Osaka, Japan) was used as the contrast agent for contrast enhanced T1WI. For DWI, we acquired a single-shot echo planar imaging sequence in a transverse plane with diffusion gradients in the x-, y-, and z-planes, with b-values between 0 and 1,000 sec/mm^2. The b-values were set following Ren *et al*. [17]. The region-of-interest (ROI) was set on an area of hyperintensity on DWI (Fig. 1), and apparent diffusion coefficient (ADC) maps were obtained. The ADCs were determined three times using a software (Functool®, GE Medical Systems, Milwaukee, WI, USA).

T2WI and FLAIR on the second day after onset showed mild hyperintensity respectively in the bilateral piriform lobes, hippocampus, and left temporal lobe, including the gyrus sylvius and gyrus ectosylvius medialis. T1WI showed iso-intensity, and post-contrast T1WI demonstrated no contrast enhancement. The lesion was described more clearly as a hyperintense focal point on DWI than on T2WI and FLAIR (Fig. 2A). The ADC values of the piriform lobes, gyrus sylvius, amygdala, gyrus ectosylvius medialis, and hippocampus were measured. The ADC values were 0.620×10^{-3} mm^2/sec in the left piriform lobe and $0.814–1.367 \times 10^{-3}$ mm^2/sec in other lesions (Table 1). The ADC value was lower on the left side than on the right side. After completing these scans, MRI was terminated because the dog started reacting to its surroundings and developed partial status epilepticus again. We suspected idiopathic epilepsy and ensuing brain damage. The dog was injected intramuscularly with 2–3 mg/kg phenobarbital (Phenobal Injection®, Fujinaga Pharm, Tokyo, Japan) and 30–40 mg/kg LEV IV three times/day. We did not administer steroids.

On the third day after onset, epilepsy had not recurred, and neurological examination suggested recovery. Body temperature had decreased to 38.6°C. The dog was sleepy but reacted well to its surroundings. No other abnormalities were observed in the neurological examination. The blood test values had improved, but not the values indicating myopathy and hypoglycemia: AST, 1,698 IU/l; ALP, 1,153 IU/l; CK; 12,143 IU/l; Glu, 56 mg/100 ml; and CRP, 7.0 mg/100 ml. Glu had increased to 94 mg/100 ml on the fourth day. We gradually reduced phenobarbital and continued with 10 mg/kg zonisamide (Excegran®, Sumitomo Dainippon Pharma, Osaka, Japan) twice/day and 20 mg/kg potassium bromide (Potassium Bromide Yamazen®, Yamazen Pharm, Osaka,

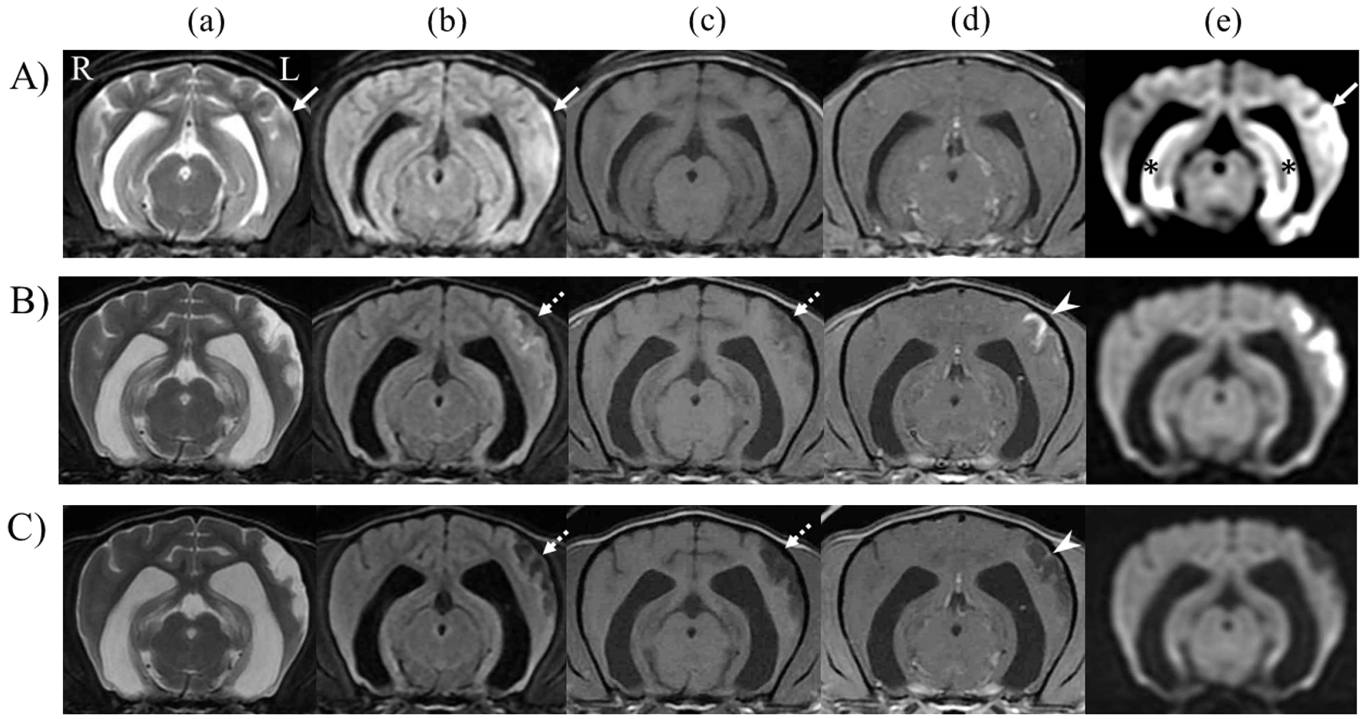

Fig. 2. Transverse images obtained at the temporal lobe level. Images were acquired on the A) second day, B) 39th day, and C) 133rd day after the epilepsy onset by a) T2WI, b) FLAIR, c) T1WI, d) post-contrast T1WI, and e) DWI. A) On the second day after onset, T2WI, FLAIR, and DWI showed hyperintensity respectively in the left temporal lobe, including the gyrus sylvius and gyrus ectosylvius medialis (arrow). T1WI showed isointensity, which was not enhanced by contrast medium. The hyperintensity was clearer on DWI than on T2WI and FLAIR, and showed in the left temporal lobe and bilateral hippocampi (asterisk). B) On day 39 after onset, the temporal lobe showed hyperintensity on T2WI. The center of the left temporal lobe showed hypointensity on FLAIR and T1WI respectively (dotted arrow). The periphery of the temporal cortex showed hyperintensity on FLAIR, with linear contrast enhancement on T1WI (arrowhead). Hyperintensity on DWI was maintained in the left temporal lobe. C) On day 133 after onset, the center of lesion in the temporal lobe showed hyperintensity on T2WI. The lesion was observed hypointensity on FLAIR and T1WI respectively (dotted arrow). The cortex periphery was hyperintense on FLAIR, with linear contrast enhancement on T1WI (arrowhead). The hyperintense lesion in the left temporal lobe was not seen on DWI. T1WI, T1-weighted imaging; T2WI, T2-weighted imaging; FLAIR, fluid attenuated inversion recovery; DWI, diffusion-weighted imaging; L, left; R, right.

Table 1. Apparent diffusion coefficient values in the piriform lobe, gyrus sylvius, amygdala, gyrus ectosylvius medialis, and hippocampus ($\times 10^{-3}$ mm^2/sec)

		Second day		39th day		133rd day	
		Ave.	SD	Ave.	SD	Ave.	SD
Piriform lobe	Left	0.620	0.008	Atrophy		Atrophy	
	Right	0.866	0.022	Atrophy		Atrophy	
Gyrus sylvius	Left	0.814	0.020	0.935	0.001	0.998	0.021
	Right	1.020	0.026	0.895	0.018	0.926	0.008
Amygdala	Left	0.869	0.040	Atrophy		Atrophy	
	Right	1.130	0.050	Atrophy		Atrophy	
Gyrus ectosylvius medialis	Left	1.013	0.006	0.955	0.076	Atrophy	
	Right	1.163	0.006	0.922	0.014	0.974	0.017
Hippocampus	Left	1.190	0.052	1.433	0.038	1.527	0.047
	Right	1.367	0.032	1.510	0.036	1.523	0.006

Diffusion-weighted imaging (DWI) was performed on the second, 39th, and 133rd day. The average (Ave.) and standard deviation (SD) were shown.

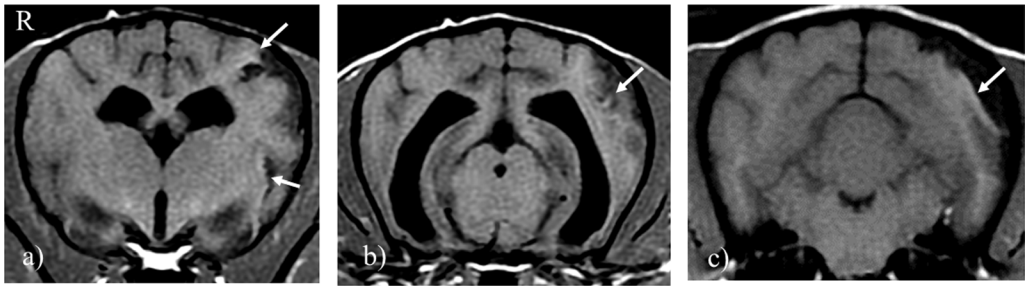

Fig. 3. The periphery of the cortical lesion on T1-weighted imaging (WI). These images showed a), b) Transverse images acquired on T1WI at the temporal lobe level on day 39 after epilepsy onset and c) Transverse image on T1WI at the occipital lobe level on day 133 after epilepsy onset. The center of lesion was hypointensity, but the periphery of the cortical lesion was hyperintense on T1WI slightly (arrow). R, right; T1WI, T1-weighted imaging.

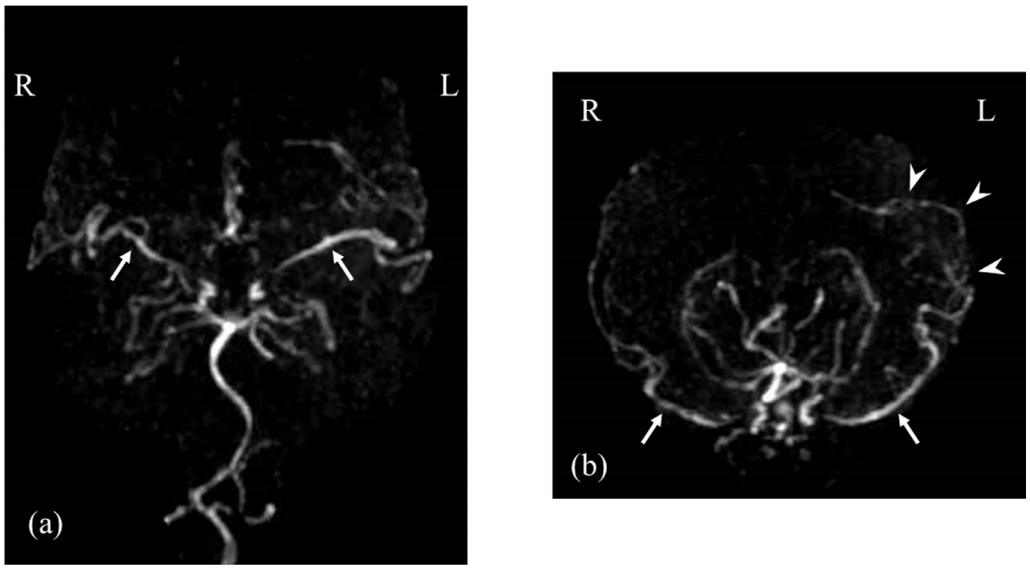

Fig. 4. Magnetic resonance angiography (MRA) on day 39 after epilepsy onset. The images show (a) ventral view, and (b) rostral view. The left middle cerebral artery was clearer than the right one (arrows). Tortuous small vessels were observed in the left temporal lobe (arrowheads). R, right side; L, left side.

Japan) once a day. Finally, phenobarbital was discontinued, and only zonisamide and potassium bromide were administered. The dog began to feed and was discharged on the 8th day, as it remained seizure-free.

On the 39th day after onset, we performed follow-up MRI and cerebrospinal (CSF) examination for differential diagnosis. The dog had normal physical and neurological examination findings and blood test results, but its behavior at home was abnormal; it demonstrated wandering and failed to excrete. MRI was performed under general anesthesia. We performed magnetic resonance angiography (MRA) as an additional scan (TR, 28 msec; TE, 6.8 msec; slice thickness, 0.8 mm; flip angle, 20°). The lateral ventricles were symmetrically dilated. The lesions in the bilateral piriform and left temporal lobes showed as hyperintense foci on T2WI (Fig. 2B). The center of the left temporal lobe was hypointense on FLAIR and T1WI, respectively. The periphery of the cortical lesion was mildly hyperintense on T1WI (Fig. 3a, 3b), with linear contrast enhancement (Fig. 2B). On DWI, hippocampus that was perceived on the second day as hyperintense, were visualized on day 39 as isointense regions. Only the left temporal lobe maintained hyperintensity (Fig. 2B). The ADC values of left temporal lobes were 0.935×10^{-3} mm^2/sec in the gyrus sylvius and 0.955×10^{-3} mm^2/sec in the gyrus ectosylvius medialis. The sites in the piriform lobes and amygdala showed atrophy, so the ADC values could not be measured. On MRA, the left middle cerebral artery was observed more clearly than the right one (Fig. 4a). Its tortuous branches were observed in the left temporal cortex (Fig. 4b). On contrast-enhanced T1WI, the diameters of the left and right middle artery were 10 and 8 mm, respectively. After the MRI investigation, a cisternal cerebrospinal fluid (CSF) tap was performed, and it showed a mild increase in protein concentration (31.6 mg/100 ml); a glial fibrillary acidic protein (GFAP) test revealed a positive finding.

We prescribed the same medication without steroids and performed a repeat MRI on the 133rd day after onset. The dog exhibited no seizure or wandering behavior and was able to respond to the owner. Physical and blood examinations showed normal

findings. MRI was acquired under general anesthesia. The brain atrophy had further progressed, and the lateral ventricles were more dilated than on the previous MRI. The temporal and the occipital lobes were hyperintense on T2WI, hypointense on FLAIR and T1WI respectively. The margins of the cerebral cortex were hyperintense on FLAIR, with linear contrast enhancement on T1WI (Fig. 2C). The center of lesion was hypointensity on T1WI, but the periphery of the cortical lesion was hyperintense slightly on non-contrast T1WI (Fig. 3c). The previously observed left temporal lobe hyperintense lesion on DWI was not seen as it had become atrophic. Although the CSF examination still tested positive for GFAP, the level had decreased to 26.9 mg/100 ml. The dog's treatment continues with antiepileptic drugs alone.

In this report, we describe a dog suspected of having hypoglycemic encephalopathy with CLN identified using DWI. In humans, DWI helps discern the cause of acute encephalopathy [10]. In typical hypoglycemic encephalopathy, CLN might occur uni- or bilateral in the cerebral cortices, hippocampi, or basal ganglia [10, 11, 19]. The CLN is seen on DWI as a hyperintense lesion that is inconsistent with the cerebral arterial territories [10, 13]. The thalami, cerebellum, and hypothalamus have a normal appearance because hypoglycemia affects the gray matter more than it affects the white matter [10]. In this report, the DWI findings were similar to those reported in humans. During the acute phase, DWI of the dog showed hyperintensity in the bilateral piriform lobes, hippocampus, and left temporal lobe. The hyperintense lesion viewed on DWI was maintained during the chronic phase by day 39. It is reported that DWI shows early neurological damage, and sustained hyperintensity on DWI suggests cell necrosis [7, 8, 12]. It is possible that the cortex lesion that maintained hyperintensity on DWI at the chronic phase in this dog showed irreversible cell damage.

In addition, during the early subacute phase, CLN shows linear hyperintensity on T1WI, and with enhanced on contrast T1WI [2, 11, 14, 19]. It is suspected that the cause is gliosis and fat-laden macrophages that react to cell damage, and the occurrence of secondary neuronal necrosis [11, 19]. As a result, the cerebral cortex protein concentration increases, leading to high signal intensity on T1WI [11, 19]. It was reported in humans that the high T1WI signal intensity continued for 11 months after onset, and the contrast-enhanced lesion on T1WI remained for up to 8 months [11]. These findings are consistent with previous reports in dogs [2, 14]. This dog supports these reports as the temporal lobe was observed as mildly hyperintense on T1WI and with enhanced on the contrast medium on days 39 and 133 after onset. The increased protein concentration and positive GFAP test result during CSF examination also indicated necrosis. In immunohistochemical analysis, CLN is reported to show an increased GFAP expression [20]. Based on MRI and CSF examination findings, it is suggested that this dog had CLN in the left temporal lobe.

It was difficult to investigate CLN causes other than hypoglycemia. As noted, CLN could also be caused by ischemic stroke, hypoxia, and seizures [2, 3, 14, 20]. DWI can be useful for distinguishing between CLN causes based on the lesion location. Infarction-caused CLN is found in the cerebral arterial territories [10]. In typical hypoxia, the damage would affect any brain region, including the cerebellum and white matter, and DWI might not show hyperintensity in the late subacute phase [10]. In this dog, DWI positioned the lesion to the cerebral cortex, so ischemic stroke and hypoxia are unlikely causes of the CLN. It is difficult to distinguish between brain damage caused by epileptic seizures and hypoglycemic encephalopathy based on DWI alone because they have a similar distribution [15]. It is possible that both were involved because the dog had hypoglycemia after epileptic seizures. In humans, MRA could be useful for hypoglycemic encephalopathy diagnosis [13]. When CLN occurs in the temporal lobe, MRA can demonstrate increased vascularity of the middle cerebral artery branches on the lesion side [13]. The cause is unknown, but it is suggested to be a compensatory change [13]. In the present report, the middle cerebral artery, which supplies the left temporal lobe, was observed more clearly than the right one, and its diameter was larger. It is said that the normal middle cerebral artery diameter in dogs is 1.0 mm, and its branches are distributed to the cerebral cortex [5]. In this dog, although the left side diameter was normal, its branches were tortuous, and more small vessels could be observed, suggesting increased vascularity.

Some MRI findings were inconsistent with previous reports in humans. In humans, the ADC values decrease in patients with hypoglycemic encephalopathy [1, 12]. According to Hartmann *et al.* [6], normal ADC values in the cerebral cortex of dogs are $0.84315 \pm 0.09824 \times 10^{-3}$ mm^2/sec [mean ± standard deviation]. In this dog, the observed ADC values were normal, except for the left piriform. They were even normal in regions suspected of being necrotic on follow-up MRI. Hypoglycemic encephalopathy might affect the ADC values. In mice, it was reported that the change in the ADC values was reversible and that the ADC values rapidly returned to normal after glucose infusion [8]. It is known that hypoglycemic encephalopathy causes the narrowing of the extracellular space. This condition differs from ischemia, which causes a shift of water from the extracellular to the intracellular domain [8]. The dog was immediately treated twice with injected 50% glucose, so it may have recovered from the severe hypoglycemia, and its ADC values returned to normal. An alternative explanation is that the ADC values were affected by necrosis. In this dog, the piriform and left temporal lobe lesions were suspected to be necrotic foci. This necrosis may have affected the ADC values when DWI was performed.

The main limitation in the present study is that we cannot confirm our diagnosis by postmortem examination because this dog is still alive. If CLN is confirmed, it will support the MRI findings.

In conclusion, we describe a dog suspected of having hypoglycemic encephalopathy with CLN. Imaging findings resembled those of CLN in humans. The lesion presented as a hyperintense slightly on T1WI and with enhanced on the contrast medium. DWI enabled early CLN lesion visualization and narrowing of the etiological possibilities. It is difficult to distinguish between seizure and hypoglycemia-induced changes because their distribution overlaps. MRA might provide further information for the differential diagnosis. DWI proved useful in detecting CLN in a dog suspected of having hypoglycemic encephalopathy.

POTENTIAL CONFLICTS OF INTEREST. The authors have nothing to disclose.

REFERENCES

1. Albayram, S., Ozer, H., Gokdemir, S., Gulsen, F., Kiziltan, G., Kocer, N. and Islak, C. 2006. Reversible reduction of apparent diffusion coefficient values in bilateral internal capsules in transient hypoglycemia-induced hemiparesis. *AJNR Am. J. Neuroradiol.* **27**: 1760–1762. [Medline]
2. Alisauskaite, N., Wang-Leandro, A., Dennler, M., Kantyka, M., Ringer, S. K., Steffen, F. and Beckmann, K. 2019. Conventional and functional magnetic resonance imaging features of late subacute cortical laminar necrosis in a dog. *J. Vet. Intern. Med.* **33**: 1759–1765. [Medline] [CrossRef]
3. Braund, K. G. and Vandevelde, M. 1979. Polioencephalomalacia in the dog. *Vet. Pathol.* **16**: 661–672. [Medline] [CrossRef]
4. du Mesnil de Rochemont, R., Neumann-Haefelin, T., Berkefeld, J., Sitzer, M. and Lanfermann, H. 2002. Magnetic resonance imaging in basilar artery occlusion. *Arch. Neurol.* **59**: 398–402. [Medline] [CrossRef]
5. Evans, H. E. and Christensen, G. C. 1922. Miller's anatomy of the dog, 2nd ed., W. B. Saunders company, Philadelphia.
6. Hartmann, A., Söffler, C., Failing, K., Schaubmar, A., Kramer, M. and Schmidt, M. J. 2014. Diffusion-weighted magnetic resonance imaging of the normal canine brain. *Vet. Radiol. Ultrasound* **55**: 592–598. [Medline] [CrossRef]
7. Hasegawa, D., Orima, H., Fujita, M., Nakamura, S., Takahashi, K., Ohkubo, S., Igarashi, H. and Hashizume, K. 2003. Diffusion-weighted imaging in kainic acid-induced complex partial status epilepticus in dogs. *Brain Res.* **983**: 115–127. [Medline] [CrossRef]
8. Hasegawa, Y., Formato, J. E., Latour, L. L., Gutierrez, J. A., Liu, K. F., Garcia, J. H., Sotak, C. H. and Fisher, M. 1996. Severe transient hypoglycemia causes reversible change in the apparent diffusion coefficient of water. *Stroke* **27**: 1648–1655, discussion 1655–1656. [Medline] [CrossRef]
9. Kim, S. Y., Goo, H. W., Lim, K. H., Kim, S. T. and Kim, K. S. 2006. Neonatal hypoglycaemic encephalopathy: diffusion-weighted imaging and proton MR spectroscopy. *Pediatr. Radiol.* **36**: 144–148. [Medline] [CrossRef]
10. Koksel, Y., Benson, J., Huang, H., Gencturk, M. and McKinney, A. M. 2018. Review of diffuse cortical injury on diffusion-weighted imaging in acutely encephalopathic patients with an acronym: "CRUMPLED". *Eur. J. Radiol. Open* **5**: 194–201. [Medline] [CrossRef]
11. Komiyama, M., Nishikawa, M. and Yasui, T. 1997. Cortical laminar necrosis in brain infarcts: chronological changes on MRI. *Neuroradiology* **39**: 474–479. [Medline] [CrossRef]
12. Lee, B. W., Jin, E. S., Hwang, H. S., Yoo, H. J. and Jeong, J. H. 2010. A case of hypoglycemic brain injuries with cortical laminar necrosis. *J. Korean Med. Sci.* **25**: 961–965. [Medline] [CrossRef]
13. Lim, C. C., Gan, R., Chan, C. L., Tan, A. W., Khoo, J. J., Chia, S. Y., Kao, S. L., Abisheganaden, J. and Sitoh, Y. Y. 2009. Severe hypoglycemia associated with an illegal sexual enhancement product adulterated with glibenclamide: MR imaging findings. *Radiology* **250**: 193–201. [Medline] [CrossRef]
14. Mariani, C. L., Platt, S. R., Newell, S. M., Terrell, S. P., Chrisman, C. L. and Clemmons, R. M. 2001. Magnetic resonance imaging of cerebral cortical necrosis (polioencephalomalacia) in a dog. *Vet. Radiol. Ultrasound* **42**: 524–531. [Medline] [CrossRef]
15. Mellema, L. M., Koblik, P. D., Kortz, G. D., LeCouteur, R. A., Chechowitz, M. A. and Dickinson, P. J. 1999. Reversible magnetic resonance imaging abnormalities in dogs following seizures. *Vet. Radiol. Ultrasound* **40**: 588–595. [Medline] [CrossRef]
16. Rajasekharan, C., Jithesh, B. and Renjith, S. W. 2013. Cortical laminar necrosis due to hypoglycaemic encephalopathy:-images in medicine. *BMJ Case Rep.* **2013**: bcr2012007726. [Medline] [CrossRef]
17. Ren, S., Chen, Z., Liu, M. and Wang, Z. 2017. The radiological findings of hypoglycemic encephalopathy: A case report with high b value DWI analysis. *Medicine (Baltimore)* **96**: e8425. [Medline] [CrossRef]
18. Shimada, A., Morita, T., Ikeda, N., Torii, S. and Haruna, A. 2000. Hypoglycaemic brain lesions in a dog with insulinoma. *J. Comp. Pathol.* **122**: 67–71. [Medline] [CrossRef]
19. Siskas, N., Lefkopoulos, A., Ioannidis, I., Charitandi, A. and Dimitriadis, A. S. 2003. Cortical laminar necrosis in brain infarcts: serial MRI. *Neuroradiology* **45**: 283–288. [Medline] [CrossRef]
20. Thomsen, B. B., Gredal, H., Wirenfeldt, M., Kristensen, B. W., Clausen, B. H., Larsen, A. E., Finsen, B., Berendt, M. and Lambertsen, K. L. 2017. Spontaneous ischaemic stroke lesions in a dog brain: neuropathological characterisation and comparison to human ischaemic stroke. *Acta Vet. Scand.* **59**: 7. [Medline] [CrossRef]